MINI REVIEW

Cibalackrot-type compounds: Stable singlet fission materials with aromatic ground state and excited state

Weixuan Zeng[1] | Dariusz W. Szczepanik[2,3] | Hugo Bronstein[1,4]

[1]Department of Chemistry, University of Cambridge, Cambridge, UK

[2]Department of Theoretical Chemistry, Faculty of Chemistry, Jagiellonian University, Kraków, Poland

[3]Institut de Química Computacional i Catàlisi and Departament de Química, Universitat de Girona, Girona, Spain

[4]Cavendish Laboratory, University of Cambridge, Cambridge, UK

Correspondence

Hugo Bronstein, Department of Chemistry, University of Cambridge, Cambridge CB2 1EW, UK.
Email: hab60@cam.ac.uk

Funding information

National Science Centre, Poland, Grant/Award Number: 2021/42/E/ST4/00332; EPSRC, Grant/Award Number: EP/S003126/1; Marie Skłodowska-Curie, Grant/Award Number: 886066

Abstract

Singlet fission is a multiexciton generation process, where one singlet exciton is absorbed and two triplet excitons are produced. The potential of more efficient photovoltaic devices utilizing singlet fission materials has attracted wide interests for tuneable, stable organic chromophores with suitable excited-state ordering. The strict energetic requirements hinder the exploration of novel organic materials, and most well-known singlet fission materials, linear acenes, are considered to be unstable in their excited states. To solve the stability issue, excited-state aromaticity provides a feasible research option, from which a few chromophores have been designed and studied. This review describes indolonaphthyridine (IND) derivative chromophores and discusses their ability to undergo singlet fission with superior ambient stability. Deepened theoretical analysis taking into account the excited-state Hückel-aromatic and diradical characters rationalizes the special properties of these chromophores. Moreover, the improved understanding of the aromatic character enables us to outline a feasible design strategy suitable for other scaffolds undergo singlet fission and excited-state aromaticity. Hopefully, this review can light a fire on the way toward various novel singlet fission chromophores designed based on the excited-state aromatic view.

KEYWORDS

aromaticity, singlet fission

1 | INTRODUCTION

Singlet exciton fission (singlet fission [SF]) in organic molecules has the potential to significantly improve the efficiency of photovoltaics. The theoretical limit of a typical single-junction solar cell can potentially be increased from ~33% to ~45% by a SF process,[1] which allows up to 200% quantum efficiencies as absorbing a single higher energy photon that generates two triplet excitons via a spin-allowed singlet exciton splitting.[2,3] In order to

achieve this, the lowest triplet (T_1) energy levels ($E(T_1)$) must approach half the energy of the lowest excited singlet state (S_1); thus, a big energy gap between S_1 and T_1 is inevitable in a SF material. The strict energetic requirement hinders the development of SF chromophores, design rules that allow for the identification, and synthesis of new SF chromophores is therefore arguably one of the most important challenges in functional organic materials research today. However, the fact that linear acenes remain the most successful chromophore for use

in SF photovoltaics, despite their well-documented instability,[4,5] demonstrates that more work must be done to understand the underlying design principles.

Aromaticity is one of the most widely applied concepts within organic chemistry.[6,7] It plays a role in the rationalization of a range of chemical properties, including stability and energy gap in both ground state and excited state. Aromaticity comes in different forms, among which the Hückel and Baird aromaticity can well fit the organic semiconducting materials with planar (or quasi-planar) structure.[7] However, neither the "perfect" Hückel's aromaticity nor Baird's aromaticity is preferred to the requirement for stable SF materials as the antiaromatic phase of them would cause a sacrifice to stability.[8] The Hückel's aromaticity system enlarges the S_0-T_1 gap (gap between ground state, S_0, and the low-lying triplet state, T_1) that raises the bar for an even larger S_1-T_1 gap, whereas the Baird's aromaticity system tends to another extreme that the S_0-T_1 gap is too small to prevent energy loss via internal conversion (IC) process to ground state. Besides, it is generally known as an either-or situation that if a compound exhibits ground-state aromaticity, then it should be antiaromatic in its excited states, and vice versa. Researchers have also attempted to manipulate singlet and triplet energetics in a similar manner within the acenes.[9,10] However, except for some linear acenes, most of the SF materials with complicated fused ring structure cannot be regarded as typical aromatic models.[11] Therefore, to rationalize the relationship between the chemical structure and photochemical properties, insights with quantitative analysis instead of "either-or" judgments are needed. The analysis can in turn help better understand and design the molecules achieving preferred performances.

In this mini review, we discuss recently reported SF chromophores suggested to be aromatic in both ground state and low-lying excited state and give an overview of our research into the quantum chemical analysis from the aromaticity aspect. Focused on the indolonaphthyridine (IND) derivative chromophores, we explored their potentials for undergoing SF and comparative advantage in stability. Further, quantum chemical analysis enables a feasible design strategy for a type of stable SF chromophores benefited from the Hückel's aromaticity. This design strategy provides an option of view to rationalize other reported chromophores with similar properties, of which the limitation and pitfalls have also been delimited.

2 | CHROMOPHORES AND EXPERIMENTAL PROPERTIES

As mentioned, to be energetically able to undergo SF, a candidate compound must exhibit an $E(S_1)/E(T_1)$ equal to or more than two. Cibalackrot as one of the IND derivatives was identified to exhibit low-lying $E(T_1)$s, which is observed in our previous studies and indicates good potential of these compounds for the applications in SF.[12,13] TD-DFT//B3LYP/6-311G** calculations on various IND cores led us to discover compounds with thiophene substituents exhibit $E(S_1)/E(T_1)$ as high as 2.38, improving on potential for exothermic SF process for their benzene-substituted equivalents (i.e., cibalackrot, $E(S_1)/E(T_1) = 1.96$ at the same level).[14] Informed by these calculations, we designed and synthesized a family of INDT molecules with chemical functionalization at the 6,6′-positions of the indigoid ring, substituents of H, F, Cl, Br, and CN were introduced as X-INDTs and an asymmetric mononitrile/monobromo compound, namely, **CNBr-INDT** was also synthesized and analyzed (Figure 1A).[15]
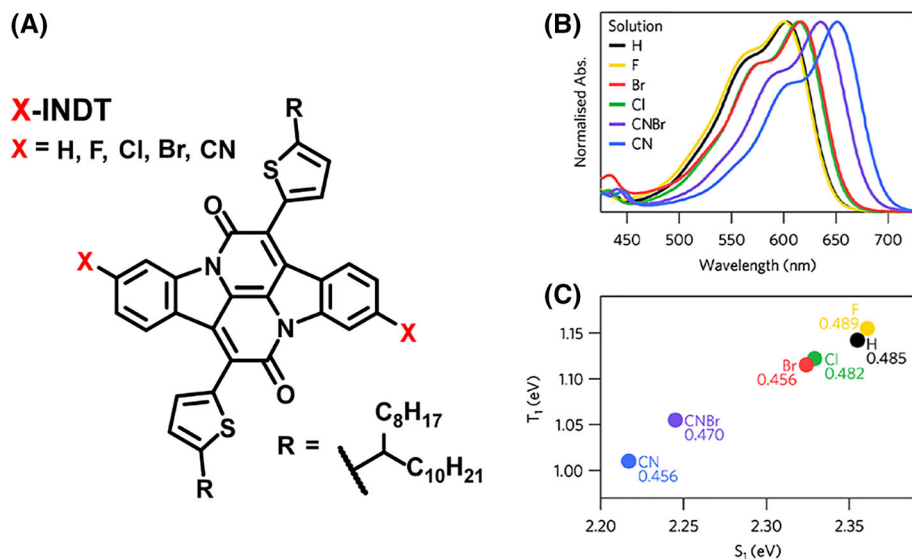
FIGURE 1 (A) Chemical structures of X-INDT with various substituents at the 6,6′-positions of the indigo rings. (B) Absorbance spectra of the X-INDT series in chloroform dilute solution. (C) $E(S_1)$ versus $E(T_1)$ with the ratios of $E(T_1)/E(S_1)$ as inset numbers (eV, TD-DFT/TDA//B3LYP/6-311++G**).[15] (*Source*: Reproduced permission is needed. Copyright © 2019, American Chemical Society.)

The effects of the different substituents for the family of materials were observed as variety in $E(S_1)$ in the solution steady-state absorbance spectra and correlated well with the calculated excited-state energies. The observed λ_{max} ranged from 602 (for **H-INDT** and **F-INDT**) to 650 nm (for **CN-INDT**), as the theoretical $E(S_1)$s ranged from 2.36 (for **H-INDT** and **F-INDT**) to 2.22 eV (for **CN-INDT**) and similar scale for the $E(T_1)$s from 1.16 to 1.01 eV (Figure 1B). The discussion here focusses on **Br-INDT** and **CN-INDT** for their properties in thin films and further investigation about the ability of undergoing SF. The observed λ_{max} for **Br-INDT** shifted from 617 nm in solution to 556 nm in film, whereas for **CN-INDT**, the shift was observed from 651 nm in solution to 541 nm in film. The shifted indicates significant intermolecular interactions between chromophores, which could be assigned to the H-type exciton coupling in films. From transient absorption spectroscopy in the nanosecond to microsecond time scale (Figure 2A), photoinduced absorptions were observed at ~680 (**Br-INDT**) and ~740 nm (**CN-INDT**) that persisted to the microsecond regime, and the triplet exciton spectral signatures were recorded by solution sensitization methods (Figure 2B, green dash). After taking into account differences in ground-state bleach and a slight bathochromic shift of the $T_1 \rightarrow T_n$ transition in the solid state, we confidently assigned these species to triplet excitons.

Electron paramagnetic resonance (EPR) spectroscopy with sublevel populations of the triplet states can further distinguish whether these triplets were formed via SF or intersystem crossing (ISC). Because SF is a bichromophoric process, dilute frozen solutions of these INDT molecules will not be able to undergo SF. Any observed zero-field sublevel populations of triplet state in dilute solution would therefore arise only from the ISC process. As expected, triplet exciton formation via ISC pathways was observable in both materials with emission/absorption polarization patterns EEEAAA under these conditions. In contrast, in the film state where the molecules aggregated and activated the inter-molecular process, SF is possible and may outcompete ISC. The EPR on thin films of the INDT compounds exhibited completely different polarization patterns comparing those in solution, namely, EAEAEA polarization for Br-INDT and AEEEAE for CN-INDT, which indicated the present of extra components with different zero-field splitting parameters and can be assigned as signature of triplet pairs formed via SF in the film state (Figure 2C).[16]

The combination of the EPR and TA spectroscopy proved conclusively that SF is an active excited-state phenomenon in the INDT chromophores. A trend in increasing triplet yield produced by the exothermicity SF in the order H < F < CNBr ≈ Cl < Br < CN as the X-substituents for the INDTs. Additionally, the INDT derivatives displayed remarkable photostability comparing with TIPS-pentacene, which is one of the most well-known SF materials. The thin film of TIPS-pentacene
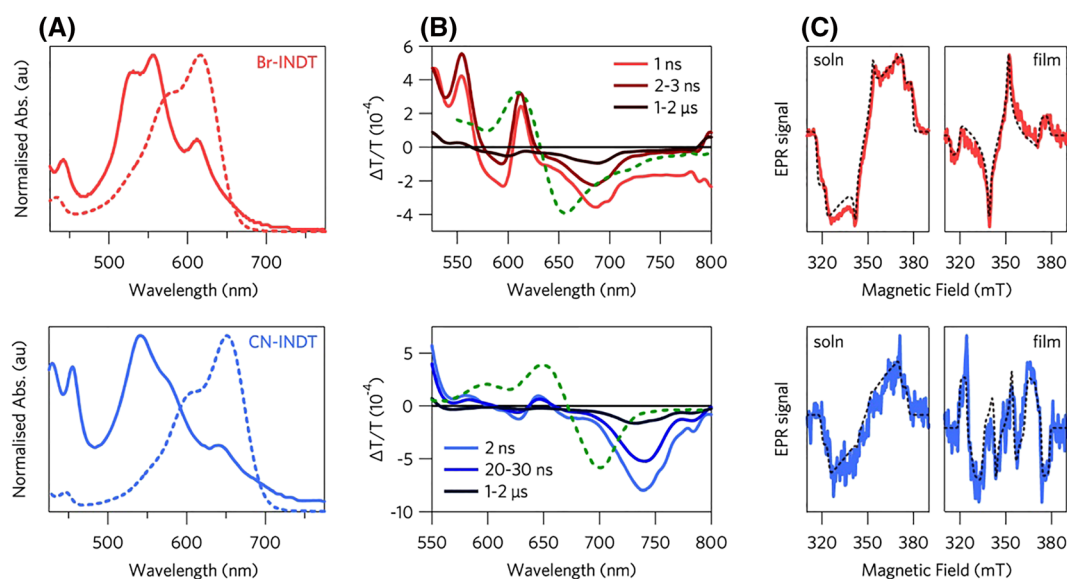

FIGURE 2 (Top, red) **Br-INDT** and (bottom, blue) **CN-INDT**: (A) Solution (dashed line, chloroform) and thin-film (solid line) steady-state absorption spectra. (B) Thin-film transient absorption spectra acquired on nanosecond to microsecond time scale following 1 ns excitation pulses at 532 nm. Solution sensitized triplet signatures shown as green dashed line. (C) Experimental (colored) and simulated (black dash) TR-EPR spectra obtained at 10 K in dilute solution (soln, left) and drop-cast films (film, right).[15] (Source: Reproduced permission is needed. Copyright © 2019, American Chemical Society.)

degrades totally after 4 days, whereas a thin film of **CN-INDT** retained over 85% activity after 31 days under the same conditions (Figure 3).

3 | THEORETICAL ANALYSIS ON THE SCAFFOLD

The remarkable photostability and the potential of undergoing SF have made the cibalackrot chromophore an attractive candidate for the application in SF photovoltaics, which also encouraged us to further explore the refined design rules on this scaffold for tailoring of molecules to better fit the requirements for SF photovoltaics.

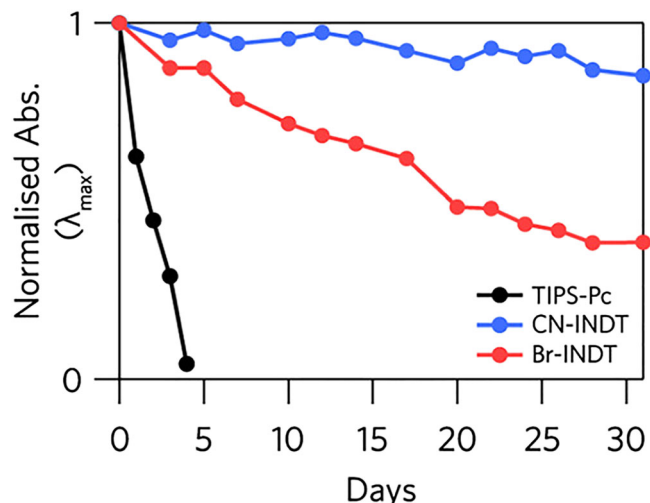A rigorous theoretical analysis of 9920 IND compounds (varied in the substituents and the flanking aromatic rings) furnished several thousand potential candidates and indicated the potential design space where the S_1-T_1 energy gap can be tuned over a large range. The red bar cut along with the $E(S_1) = 2.1$ eV, with the $E(T_1)$s ranged from about 0.7 to 1.5 eV, and with the relevant $E(S_1)/E(T_1)$ spanned from 3.0 to 1.4 (on TDDFT [TDA]/B3LYP/6-311++G**), which is crucial for the energetic requirement of exothermic SF process. I–III IND compounds represent typical models with low, middle, and high $E(T_1)$ through the red bar (Figure 4), which share the same IND chromophore core but vary in the outer rings (marked as pink), heterocycles, and/or substituents. The trend of the $E(T_1)$s was observed to be connected with the calculated nucleus-independent chemical shift (NICS)[17] values of the pyrrole-like five member rings (non-marked as white) in the chromophores at the T_1 state, shining a light on a feasible understanding of the special properties of the IND compounds from the excited-state aromaticity view. Interestingly, a recent work by Weber and Mori identified about 400,000 derivatives with the cibalackrot as the foundational scaffold to be SF candidates out of four million indigoid derivatives introducing machine learning-assisted quantum chemistry.[18] Direct correlations between the energy requirement of SF, the biradical character, and the charge and triplet spin density were systemically examined by purely data-driven extraction methods. This work not only provides an efficient way to construct databases of millions of molecules and screen for candidate for a certain requirement, such as energetic condition of SF process, but also helps unveiling the unexplored correlations with specific properties with the large databases.

Inspired by above results, we conducted more comprehensive theoretical analysis on the IND scaffold to further explore and try to develop refined design rules for the tailoring of molecules to better function as materials for SF photovoltaics based on the aromaticity view.

The first task is to dissect the effects of the aromaticity in both S_0 and T_1 of the parent IND molecule
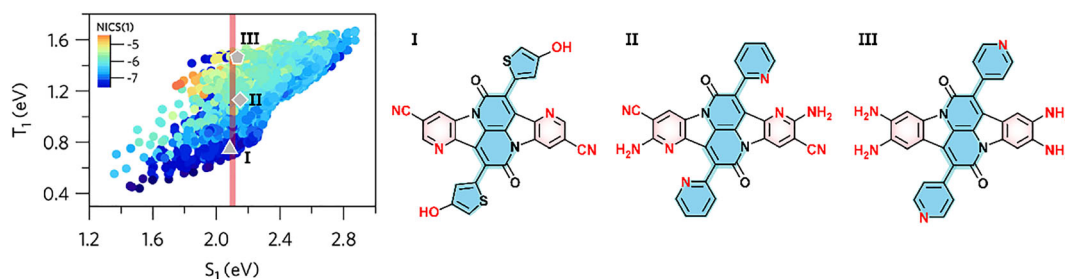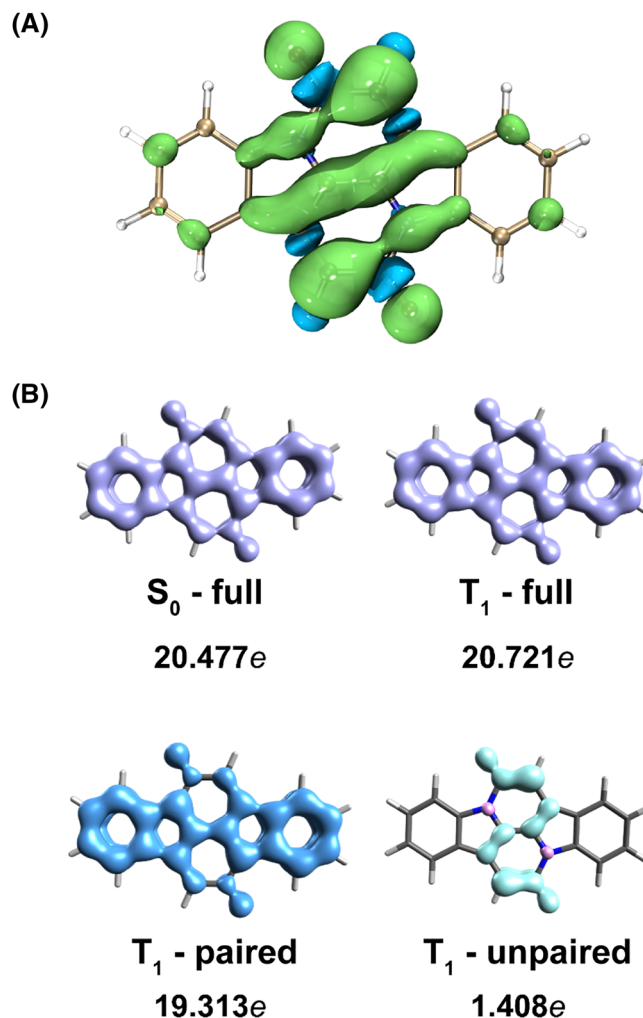

FIGURE 3 Normalized intensity of the λ_{max} of the steady-state absorbance spectra of thin films of TIPS-pentacene (**TIPS-Pc**), **Br-INDT**, and **CN-INDT** spun from 5 mg/ml solutions in chloroform over 31 days.[15] (*Source*: Reproduced permission is needed. Copyright © 2019, American Chemical Society.)

FIGURE 4 Calculated $E(S_1)$ and $E(T_1)$ for 9920 candidates with the corresponding C5 NICS(1) shown in the color map. Red bar shows $E(S_1) = 2.1$ eV, chemical structures of three models picked from the red bar on the right.[15] (*Source*: Reproduced permission is needed. Copyright © 2019, American Chemical Society.)
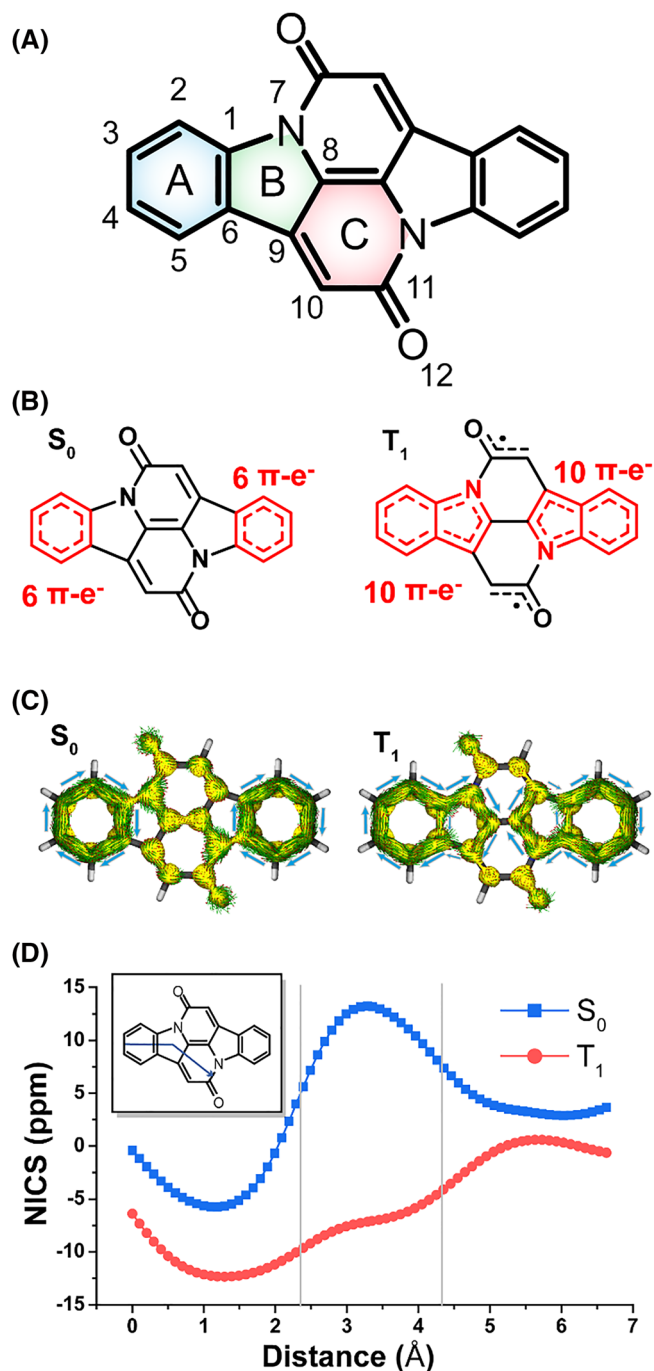
FIGURE 5 (A) Chemical structure of indolonaphthyridine-6,13-dione (**CIBA**), the relevant atoms and rings in symmetric positions are signed with an apostrophe. (B) Hückel-aromatic units are marked as red: two benzene units in the S_0 state and two indole units in the T_1 state. (C) π-Electron ring currents according to AICD and (D) π-NICS-*XY* scan in the S_0 and T_1 states of **CIBA** (GIAO/(U)B3LYP/6-311+G**//(U)B3LYP/6-311+G**).[19] (*Source*: Reproduced permission is needed. Copyright © Royal Society of Chemistry.)

FIGURE 6 (A) Spin density distribution in the T1 state of CIBA ($\rho = 0.0008$) and (B) EDDB$_H$ isosurfaces ($\rho = 0.006$) with the corresponding electron populations in the S_0 state and in the T_1 state (total and dissected into paired and unpaired electron components) ((U)B3LYP/6-311+G**).[19] (*Source*: Reproduced permission is needed. Copyright © Royal Society of Chemistry.)

(Figure 5A, the parent cibalackrot, **CIBA**) with the main question of is there aromaticity; and if yes, which rings contribute and what type of aromaticity is it? Referring to its symmetry, the **CIBA** was marked separately as A, B, and C rings with numbers for relevant atoms for later-on discussion. The magnetic indices, π-electron-only anisotropy of the induced current density (AICD)[20] and NICS-*XY* scans, proved intuitive overall; the geometric harmonic oscillator model of aromaticity (HOMA),[21] the electronic aromatic fluctuation (FLU),[22] and multicenter indice (MCI)[23] give corroborations on each specific rings. Supported by all above aromaticity indices, the two benzene rings (A/A′) with six π-electrons are signed Hückel aromatic in both S_0 and T_1 states. The aromatic region extends to the pyrrole-like five member rings (B/B′) and forms indole-like 10 member rings (AB/A′B′) with 10 π-electrons in T_1 state, which can also be marked Hückel-aromatic features. On the contrary, the CC′
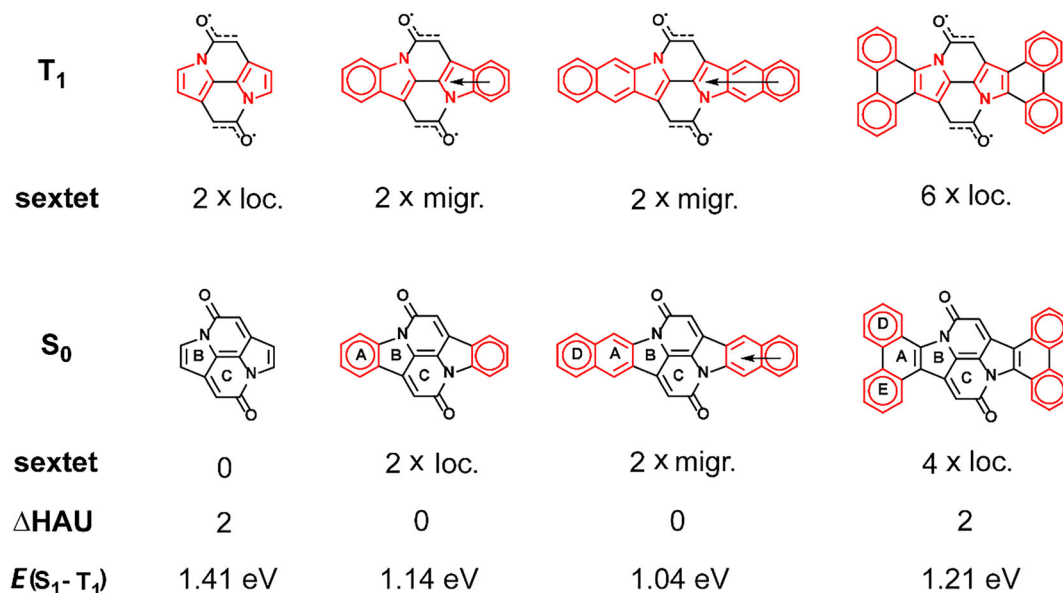
moiety exhibits fewer aromatic features and is best described as nonaromatic in both S_0 and T_1 states (Figure 5C,D).

To identify the type of aromaticity, that is, Hückel-, Baird, or Hückel-Baird hybrid type, in the complicated fused ring, we analyzed the ratios between the difference in spin-separated FLU values ($\Delta FLU_{\alpha\beta}/FLU$, where $\Delta FLU_{\alpha\beta} = FLU_\alpha - FLU_\beta$) as the $\Delta FLU_{\alpha\beta}$ is zero or negligible in a Hückel-aromatic ring, whereas it exhibits a nonzero value in a Baird-aromatic ring.[24] The quantitative results also enable us to identify those features in-between Hückel and Baird aromaticity, so call hybrid type. Nearly zero ratio reveal the Hückel-aromatic characters of the A/A′ rings at S_0, AB/A′B′ ring at T_1 in **CIBA**. The indole-like AB moiety at T_1 exhibits very similar aromatic character comparing to a 10 π-electron Hückel-aromatic indole, which further confirm the **CIBA** in its T_1 is Hückel aromatic dominated by the AB/A′B′ rings, not Baird aromatic contributed only by B/B′ five member rings.

The central CC′ segment has nonaromatic features in its S_0 and T_1; then, how do the substituents on the C_α atoms function to tune the properties of the chromophores? The spin density distribution shows that the triplet diradical character is mainly within the CC′ unit. The heavy-atom-only electron density of delocalized bonds ($EDDB_H$) method[25] further confirms the effect of enhanced π-conjugation by unpaired electrons within the CC′ moiety (Figure 6).

We concluded from above results that the excited state of **CIBA** is mainly contributed by the indole-like AB ring with Hückel-aromatic characters, whereas the diradical character focuses to the central CC′ ring. Based on this, the method to fine-tune the excited-state energy levels was explored. Substituents on the C_α atoms in the CC′ ring documented their effects on the unpaired spin density distributed on the framework, by which the $E(S_1)$ and $E(T_1)$ can be tuned similarly with good linear trends. These trends require that the S_1 and T_1 states are described similarly by the same electron configuration (except for the multiplicity difference), and the exchange interaction is constant throughout the set of molecules.

Benzannelation on the Hückel-aromatic peripheral AB/A′B′ rings represent one of the drivers for further tailoring the energy difference between the S_1 and T_1 states, which has direct effect on the aromatic character of the scaffolds. Clar's sextet were introduced for better descriptions of the benzannelated models as one can count the number of those sextets and figure out the difference between the S_0 and the diradicaloid T_1 form, which leads an intuitive understanding of the excited-state energies. Notably, the aromatic features of the predicted Clar's sextets were further proved comprehensively by various perspectives of aromatic indexes mentioned earlier. Difference of S_1-T_1 splittings on the benzannelated models of 0.17 eV was observed, which can well fit their aromatic features though the magnitude of the S_1-T_1

T_1				
sextet	2 × loc.	2 × migr.	2 × migr.	6 × loc.
S_0				
sextet	0	2 × loc.	2 × migr.	4 × loc.
ΔHAU	2	0	0	2
$E(S_1$-$T_1)$	1.41 eV	1.14 eV	1.04 eV	1.21 eV

FIGURE 7 Chemical structure of benzannelated models, the relevant atoms and rings in symmetric positions are signed with an apostrophe. Red units represent cycles which are Clar's sextets in the S_0 and T_1 states, respectively. ΔHAU refers to the difference number of Hückel-aromatic sextet units in relevant states (T_1-S_0). $E(S_1$-$T_1)$ is the S_1-T_1 splitting energy based on vertical excitation (TD-DFT//M06-2X/def2-SVP). (*Source*: Reproduced permission is needed. Copyright © Royal Society of Chemistry.)

splitting is not constant across the series of the models (Figure 7).

Now looking back upon the IND series presented at the beginning of this section, we can rationalize the "dramatic" difference in their excited-state energy levels using the aforementioned hypothesis on the CIBA-type scaffold. The π-conjugation through the central CC′ rings were significantly affected by the substituents. Thiophenyl substituents on compound I afford better conjugation, comparing with the pyridines on compounds II and III for the steric hindrance. Compound I therefore exhibits three times larger ratio of spin density on the substituents (over 35%) compared with compounds II and III (about 10%), which results in much lower $E(T_1)$. The energy difference between compounds II and III should be assigned to the Hückel-aromatic peripheral AB/A′B′ rings; besides, the different substituents the Hückel-aromatic A/A′ rings are less aromatic pyridines in II and more aromatic benzenes in III, and these should dominate the excited-state energies.

4 | EXTENSION AND LIMITATION OF THE DESIGN APPROACH

Having investigated the CIBA-type scaffold, the design approach to tune the excited-state energies can be outlined as (i) choice of substituents at C_α atoms and (ii) benzannelations and other modifications on the peripheral aromatic rings. In this section, we will extend the design approach to a broader range of various types of chromophores (Figure 8).

Dipyrrolonaphthyridinedione (**DPND**) is another example of an SF material reported to be with high photostability both in excited triplet and singlet states, which is suggested to be benefited from its Baird-aromatic character in triplet state.[26] The aromaticity in its T_1 was well documented, and the further analysis on the pyrrole-like five member rings about the $\Delta FLU_{\alpha\beta}/FLU$ value of -0.803 shows the contribution of Hückel-Baird hybrid type (Table 1). Because the spin density was highly contributed by the central rings, changing the substituents on these sites can feasibly tuning the $E(T_1)$s and the ratios of $E(S_1)/E(T_1)$ as well. Another example is the hydrocarbon material styryl-substituted dibenzopentalen (**SDP**), which was reported to be with intramolecular SF and good photostability.[27] The **SDP** also fits well within the outlined design rule that the Hückel-aromatic peripheral rings can contribute to the stability in both ground state and excited state, but the styryl substituents efficiently delocalized the spin density of the unpaired electrons.

We noticed the framework does not fit when the styryls are removed, leaving only the dibenzopentalen (**DP**) core. Except for the NICS values, the other aromatic indexes of the peripheral rings indicate less aromatic in T_1 state, which is different from those of **SDP**. Besides, the central pentalene-like rings were suggested to be 4n-π contribution, of which the aromatic features were further analyzed by NICS-*XY* scan to be a bit antiaromatic on the
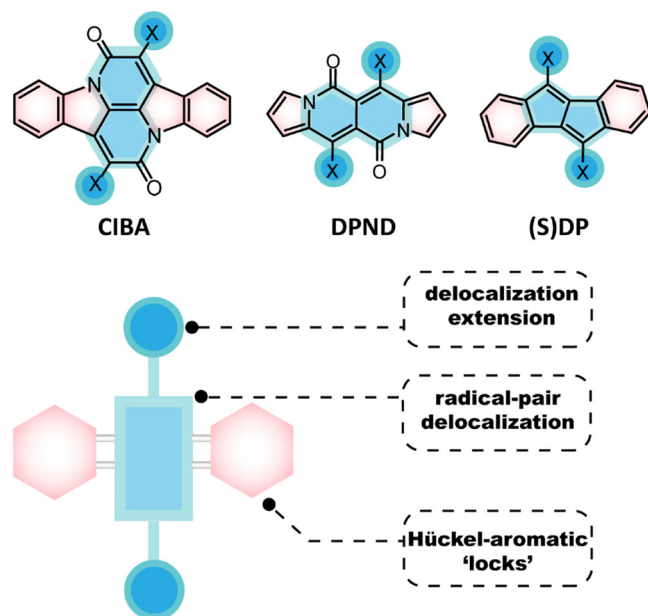

FIGURE 8 Chemical structure of SF chromophores (top) and an outline graph of the design approach (bottom)

TABLE 1 Values of key aromatic indices for the peripheral aromatic cycles in various chromophores

	S_0				T^a				
	π-NICS$_{ZZ}$	MCI	HOMA	FLU	π-NICS$_{ZZ}$	MCI	HOMA	FLU	$\Delta FLU_{\alpha\beta}/FLU$
CIBA	−5.8	0.053	0.924	0.003	−12.3	0.048	0.898	0.005	0.307
DNPD	−20.5[a]	0.028	0.852[a]	0.003	−14.3[a]	0.020	0.797[a]	0.006	−0.803
DP	−11.0	0.054	0.926	0.003	−12.0	0.026	0.612	0.013	−0.590
SDP	−9.8	0.053	0.932	0.002	−7.3	0.048	0.922	0.003	0.183

[a]NICS(1)$_{zz}$ and HOMA values are extracted from Jorner et al.[26]

ground state and become aromatic in its T_1. These results again emphasize the importance of comprehensive analysis for the aromaticity, one cannot simply conclude from any index solely. In **SDP**, the central pentalene-like rings remain almost nonaromatic both in S_0 and T_1 states. The different features result from the different spin density distribution of **DP** and **SDP**, as it distributed through the fused rings of **DP** backbone while mainly going through the styryl substituents in **SDP**.

Also to be noted, the excited energy is one of the complicated requirements for undergoing SF, especially in the solid state that is commonly used for the applications in devices based on organic semiconducting materials. Cibalackrot-type compounds (or others) might not be to undergo SF processes when simply changing the substituents, due to either incorrect electronic coupling between adjacent chromophores or from specific packing arrangements affecting the excited-state energies.[28]

5 | CONCLUSION

In this mini review, we summarize our exploration to the photostable SF materials benefited from aromaticity in both ground state and excited state. Taking the indolonaphthyridine chromophore as a pointcut, we exploited the ability of undergoing SF while exhibiting superior stability in excited states for the indolonaphthyridine thiophenes. Further analysis of the scaffold revealed the Hückel-, instead of Baird-aromatic characters in both ground state and low-lying triplet states, and the unpaired electrons are delocalized mainly through the central core. Based on the understanding, we outlined a design approach to tuning the excited-state energy levels by changing the substituents at the site of greatest spin density and modifying the aromatic rings of the scaffold. This approach can be further adapted to various novel SF chromophores with similar framework and therefore useful for seeking new candidates for undergoing SF. These results also emphasize the importance of more comprehensive understanding of the nature of the excited-state aromaticity and avoiding the risk of overuse of the Baird-aromaticity concept to molecules misleading by solely indexed evidence.

ACKNOWLEDGMENTS

CONFLICTS OF INTEREST

The authors declare that the research was conducted in the absence of any commercial or financial relationships that could be construed as a potential conflict of interest.

ORCID

Hugo Bronstein https://orcid.org/0000-0003-0293-8775

REFERENCES

[1] A. Rao, R. H. Friend, *Nat. Rev. Mater.* **2017**, *2*, 17063.
[2] M. Einzinger, T. Wu, J. F. Kompalla, H. L. Smith, C. F. Perkinson, L. Nienhaus, S. Wieghold, D. N. Congreve, A. Kahn, M. G. Bawendi, M. A. Baldo, *Nature* **2019**, *571*, 90.
[3] T. Ullrich, D. Munz, D. M. Guldi, *Chem. Soc. Rev.* **2021**, *50*, 3485.
[4] B. H. Northrop, K. N. Houk, A. Maliakal, *Photochem. Photobiol. Sci.* **2008**, *7*, 1463.
[5] S. S. Zade, N. Zamoshchik, A. R. Reddy, G. Fridman-Marueli, D. Sheberla, M. Bendikov, *J.Am. Chem. Soc.* **2011**, *133*, 10803.
[6] H. Ottosson, *Nat. Chem.* **2012**, *4*, 969.
[7] M. Rosenberg, C. Dahlstrand, K. Kilså, H. Ottosson, *Chem. Rev.* **2014**, *114*, 5379.
[8] O. El Bakouri, J. R. Smith, H. Ottosson, *J.Am. Chem. Soc.* **2020**, *142*, 5602.
[9] M. Pinheiro Jr., F. B. C. Machado, F. Plasser, A. J. A. Aquino, H. Lischka, *J.Mater. Chem. C* **2020**, *8*, 7793.
[10] G. Markert, E. Paenurk, R. Gershoni-Poranne, *Chem. – Eur. J.* **2021**, *27*, 6923.
[11] D. Padula, Ö. H. Omar, T. Nematiaram, A. Troisi, *Energy Environ. Sci.* **2019**, *12*, 2412.
[12] K. J. Fallon, H. Bronstein, *Acc.Chem. Res.* **2021**, *54*, 182.
[13] M. B. Smith, J. Michl, *Annu. Rev. Phys. Chem.* **2013**, *64*, 361.
[14] S. N. Sanders, E. Kumarasamy, K. J. Fallon, M. Y. Sfeir, L. M. Campos, *Chem. Sci.* **2020**, *11*, 1079.
[15] K. J. Fallon, P. Budden, E. Salvadori, A. M. Ganose, C. N. Savory, L. Eyre, S. Dowland, Q. Ai, S. Goodlett, C. Risko, D. O. Scanlon, C. W. M. Kay, A. Rao, R. H. Friend, A. J. Musser, H. Bronstein, *J.Am. Chem. Soc.* **2019**, *141*, 13867.
[16] L. R. Weiss, S. L. Bayliss, F. Kraffert, K. J. Thorley, J. E. Anthony, R. Bittl, R. H. Friend, A. Rao, N. C. Greenham, J. Behrends, *Nat. Phys.* **2017**, *13*, 176.
[17] A. Stanger, *J. Org. Chem.* **2006**, *71*, 883.
[18] F. Weber, H. Mori, *npj Comput. Mater.* **2022**, *8*, 176.
[19] W. Zeng, O. El Bakouri, D. W. Szczepanik, H. Bronstein, H. Ottosson, *Chem. Sci.* **2021**, *12*, 6159.
[20] D. Geuenich, K. Hess, F. Köhler, R. Herges, *Chem. Rev.* **2005**, *105*, 3758.
[21] T. M. Krygowski, *J. Chem. Inf. Comput. Sci.* **1993**, *33*, 70.
[22] E. Matito, M. Duran, M. Solà, *J. Chem. Phys.* **2005**, *122*, 014109.
[23] P. Bultinck, R. Ponec, S. Van Damme, *J. Phys. Org. Chem.* **2005**, *18*, 706.
[24] L. Wang, L. Lin, J. Yang, Y. Wu, H. Wang, J. Zhu, J. Yao, H. Fu, *J.Am. Chem. Soc.* **2020**, *142*, 10235.
[25] Y. Wu, Y. Wang, J. Chen, G. Zhang, J. Yao, D. Zhang, H. Fu, *Angew. Chem., Int. Ed.* **2017**, *56*, 9400.
[26] K. Jorner, F. Feixas, R. Ayub, R. Lindh, M. Solà, H. Ottosson, *Chem.–Eur. J.* **2016**, *22*, 2793.

[27] D. W. Szczepanik, M. Andrzejak, J. Dominikowska, B. Pawełek, T. M. Krygowski, H. Szatylowicz, M. Solà, *Phys. Chem. Chem. Phys.* **2017**, *19*, 28970.

[28] J. L. Ryerson, A. Zaykov, L. E. A. Suarez, R. W. A. Havenith, B. R. Stepp, P. I. Dron, J. Kaleta, A. Akdag, S. J. Teat, T. F. Magnera, J. R. Miller, Z. Havlas, R. Broer, S. Faraji, J. Michl, J. C. Johnson, *J. Chem. Phys.* **2019**, *151*, 184903.